Local order and hybridization effects for Mn ions probed by resonant soft x-ray spectroscopies: The Mn:CdTe(110) interface revisited

L. Sangaletti,[1] A. Verdini,[2] S. Pagliara,[1] G. Drera,[1] L. Floreano,[2] A. Goldoni,[3] and A. Morgante[2,4]
[1]*Dipartimento di Matematica e Fisica, Università Cattolica, via dei Musei 41, 25121 Brescia, Italy*
[2]*Laboratorio TASC, IOM-CNR, S.S. 14, Km 163,5, I-34149 Basovizza, Italy*
[3]*Sincrotrone Trieste, S.S. 14, Km 163,5 Area Science Park, I-34149 Basovizza, Italy*
[4]*Dipartimento di Fisica, Università di Trieste,Via Valerio 2, I-34127, Italy*
(Received 26 January 2010; revised manuscript received 7 June 2010; published 25 June 2010)

The electronic structure and the local ordering of Mn:CdTe(110) interface, produced by evaporating at room temperature (RT) 2 ML of Mn on a CdTe(110) single-crystal surface, have been probed by soft x-ray spectroscopies. Strong Mn-Te hybridization effects are found both in core level and valence-band photoemission spectra. The analysis of resonant photoelectron-diffraction patterns indicates that, already at RT, Mn atoms diffuse into CdTe down to the fourth layer, replacing the isovalent Cd atoms in the lattice.

DOI: 10.1103/PhysRevB.81.245320 PACS number(s): 75.50.Pp, 61.05.js, 68.35.Fx, 79.60.−i

Mn-doped cadmium telluride is a well-known diluted magnetic semiconductor (DMS), which displays interesting magnetic properties, ranging from paramagnetism to antiferromagnetism and spin-glass behavior.[1] With respect to ferromagnetic (Ga,Mn)As, that shows a relatively high T_C and the possibility to achieve a suitable doping, (Cd,Mn)Te has traditionally been difficult to dope (e.g., nitrogen doping), and only recently claims of ferromagnetism in (Cd,Mn)Te have been reported,[2,3] which make this DMS class of materials apparently less suitable for applications. However, along with other II-VI DMS, the interest on (Cd,Mn)Te is still very high. With respect to (Ga,Mn)As, these materials and their heterostructures are relatively easy to prepare both in bulk and in thin layers. This opens the possibility to use these materials for testing new concepts for spintronic applications[4] based in particular on low-dimensional structures such as quantum wells (QWs), quantum dots, or digital alloys.[5–10]

Due to the reduced dimensionality of the Mn-doped layer [i.e., infinite extent in the *xy* plane but thickness typically below 100 Å in the *z* direction, and down to submonolayers (ML) in digital alloys[10]], the effort on the growth of QWs and superlattices (SL) requires a control of the deposition process on an atomic scale. Progresses in understanding these processes will take a strong benefit form the spectroscopic techniques that are able to probe the local environment and electronic properties of Mn atoms diluted in the semiconductor host matrix. Indeed, photoemission spectroscopies are playing an important role in the study of DMS because in resonance conditions they can provide information on the contribution of magnetic ions to the spectral weight in the valence-band region, even for a low concentration of the magnetic TM ions.[11–14]

Aim of the present study is the investigation of the local structural and electronic properties of Mn ions in a thin Mn:CdTe(110) interface prepared by Mn evaporation at room temperature (RT) on the (110) surface of a CdTe single crystal. While early evidences of Mn interdiffusion have been presented by Wall *et al.*,[15] a systematic investigation of the problem of Mn interdiffusion in CdTe, which includes a joint electronic and structural investigation, is still missing.

Rather than a direct comparison with molecular-beam epitaxy (MBE)-grown (Mn,Cd)Te samples, the main interest of our study is the formation of the Mn:CdTe interface itself. Indeed, the evaporation of sub-ML to few ML of metallic cations (e.g., Mn) on semiconductor surfaces has been largely explored in the preparation of subnanometric interfaces leading to new concepts in the interface growth and in novel magnetic interfaces. For example, the approach we follow has been recently used to investigate the Mn:Ge(111) or the Mn:Ge(100) interfaces and to explore new magnetic properties in ultrathin Mn_xGe_{1-x} interfaces.[16–19]

In particular, in order to relate the local structural properties of Mn ions to the electronic properties of the Mn:CdTe(110) interface, we have used the resonant photoelectron diffraction (RESPED) technique, a novel tool that couples the enhanced atomic selectivity of resonant photoemission with the local structural sensitivity of photoelectron diffraction.[20] By suitable choice of the deposition conditions, we have been able to produce a $Cd_{1-x}Mn_xTe$ surface alloy without detectable segregation of metallic Mn layers. This segregation-free surface alloy can also be assumed as a model of $Cd_{1-x}Mn_xTe$ ultrathin layers in SL and QW, where the understanding of Mn-diffusion mechanisms at the interface has been recognized as a major problem for a consistent description of the electronic and magnetic properties.[10,21–25] Our results demonstrate that Mn diffuses already at RT down to the fourth layer below the CdTe(110) surface, with an ordered local environment, maintaining a strong hybridization with Te states. This puts on a solid ground the early speculations on the substitution of Cd by Mn in the CdTe lattice,[15,26] and provides an experimental evidence of the capability of Mn to diffuse into the CdTe lattice. The similarity of the present spectroscopic data with those found for bulk $Cd_{1-x}Mn_xTe$ indicate that the diffusion process is rather efficient and a bulklike behavior is found also for this thin Mn:CdTe interface.

The experiments were performed at the ALOISA beam line[27] of the Elettra Synchrotron Light Source. Mn layers were deposited at room temperature by *in situ* electron-beam evaporation, following the procedure identified in a previous study.[26] Accordingly, the present experiment has been carried

 ©2010 The American Physical Society

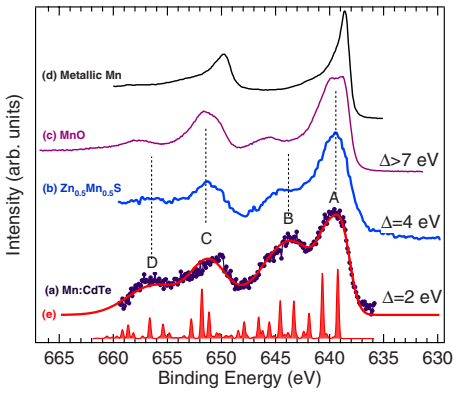

FIG. 1. (Color online) Comparison of Mn $2p$ XPS spectra from (a) Mn:CdTe(110), (b) $Zn_{1-x}Mn_xTe$ (adapted from Ref. 28), (c) MnO (adapted from Ref. 29), and from (d) a reference metallic Mn thick film deposited on a silicon wafer. (e) Calculated Mn $2p$ XPS spectrum for Mn^{2+} ion with charge-transfer derived configurations (Δ=2.1 eV, T=2.2 eV, Q=6.0 eV, and U=5.1 eV).

out at a coverage of 2 ML, i.e., below the threshold where also the metallic Mn film is found.

By subtracting from the photoemission spectrum collected after the evaporation of 2 ML the substrate contribution in the Mn $2p$ region, the spectrum of the $Cd_{1-x}Mn_xTe$ alloy is obtained (Fig. 1). For the present coverage, four spectral features are detectable, i.e., a couple of features (A and B in Fig. 1) ascribed to Mn $2p_{3/2}$ emission, and another couple at higher binding energy (BE), ascribed to the Mn $2p_{1/2}$ emission (C and D in Fig. 1). The twofold nature of each spin-orbit split component is ascribed to the strong hybridization between Mn $3d$ and Te $5p$ orbitals, which produces strong charge–transfer-related satellites, as already observed for $Zn_{1-x}Mn_xS$,[28] and more recently for $Zn_{1-x}Mn_xSe$.[30] These spectral features indicate that when Mn cations are evaporated onto the surface of the CdTe crystal, the Mn cations are found to make bonds with the nearby Te anions.

The intensity of B and D satellite peaks depends on the magnitude of the charge-transfer, CT, energy. The lower is the energy cost associated with the CT, the higher is the satellite peak intensity. In fact, the satellite peak intensity is found to increase going from the strongly insulating MnO (Ref. 29) [Fig. 1(c)] to $Zn_{1-x}Mn_xS$ (Ref. 28) [Fig. 1(b)], and finally to Mn:CdTe [Fig. 1(a)], with a corresponding decrease of the CT energy from about 7.0 eV (MnO),[31] to 4.0 eV ($Zn_{1-x}Mn_xS$) and, finally, to 2.0 eV (Mn:CdTe).

In Fig. 2(a) the results of RESPES experiment are shown as a contour plot of the measured photoemission intensity vs both the binding energy and the photon energy. For each photon energy across the Mn $2p$-$3d$ absorption edge, a valence-band photoemission spectrum has been collected. The intensity of each photoemission spectrum was normalized with respect to the incident photon flux.

The Mn $2p$ x-ray absorption spectroscopy (XAS) spectrum is shown in Fig. 2(b). This spectrum displays a fine-structure characteristic of Mn^{2+} ions in DMS,[32] arising from the multiplet terms of the $2p^53d^6$ final-state configuration of the Mn^{2+} ions diffused into the CdTe host crystal.

The possibility to carry out resonant photoemission at the

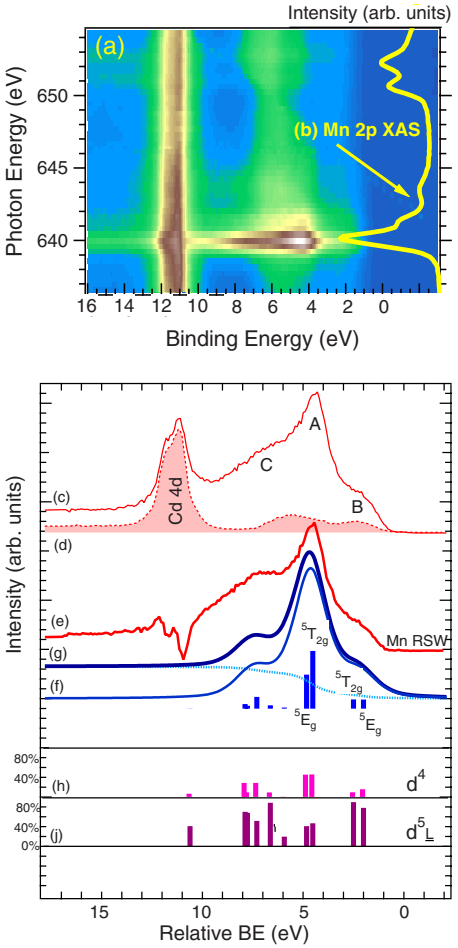

FIG. 2. (Color online) (a) Two dimensional plot of RESPES data collected from the valence-band region for different photon energies ranging from 636 to 655 eV; (b) XAS profile measured at the Mn L threshold; (e) Mn RSW obtained by subtracting from the spectrum collected at resonance (c) the spectrum collected off resonance (d). CI cluster calculations of the VB spectrum (g) obtained by adding a proper background (dotted line) to the calculated Mn $3d$ spectral weight (f). Weight of the $|3d^4\rangle$ (h) and $|d^5\underline{L}\rangle$ (j) configurations in the calculated spectrum.

Mn L edge is particularly important for DMS since it is possible to single out the contribution of the magnetic ion to the spectral valence-band spectrum. As can be observed in Fig. 2, the photoemission spectra collected across the Mn L threshold show a giant resonant behavior. In particular, an intense emission [A peak, Fig. 2(c)] is detectable at a binding energy of about 4.5 eV, with two features (B and C) on the low- and high-BE sides, respectively. The Mn contribution to the density of states in the valence band, hereafter denoted with Mn resonating spectral weight [RSW, Fig. 2(e)], has been extracted by subtracting from the resonant spectrum collected with a $h\nu$=640.5 eV photon [Fig. 2(c)] the non-resonant spectrum collected with $h\nu$=636 eV [Fig. 2(d)] Three main features A, B, and C can be detected, and the overall spectral profile is very similar to that observed for bulk $Cd_{1-x}Mn_xTe$ crystals.[13]

Impurity cluster configuration-interaction (CI) calculations of the Mn $3d$ spectral weight are shown in Figs.

2(g)–2(j). In the CI approach several configurations, denoted as d^n, $d^{n+1}\underline{L}$ ($\underline{L}$ denotes a ligand hole, here a hole on Te $4p$ orbitals) are used to describe the open shell of the $3d$ transition metal ion during the photoemission process. The spectral weight in a photoemission experiment is calculated, in the sudden approximation, by projecting the final-state configurations ($|\Psi_{i,fs}\rangle$) on the ground state, i.e., $I_{\mathrm{XPS}}(\mathrm{BE}) \propto \Sigma_i |\langle \Psi_{\mathrm{GS}} | \Psi_{i,fs} \rangle|^2 \delta(\mathrm{BE}-\varepsilon_i)$ where $|\Psi_{\mathrm{GS}}\rangle$ represents the ground-state (GS) wave function, and the sum is run over all final-state configurations $|\Psi_{i,fs}\rangle$ with energy ε_i. Where required, proper fractional parentage coefficients can be used, as was done for the valence-band calculations.

In the case of core-level photoemission we have used a full multiplet approach but we used effective (i.e., not symmetry dependent) values for charge transfer Δ and hybridization T energies. Whereas, for valence-band photoemission, we adopted the scheme proposed by Mizokawa and Fujimori.[33] For core-level photoemission, the spectrum displayed in Fig. 1 was obtained by setting the CT energy $\Delta = 2.1 \pm 0.5$ eV, the hybridization integral $T = 2.2 \pm 0.25$ eV, the core-hole $3d$ electron Coulomb attraction $Q_{pd} = 6.0 \pm 0.5$ eV, and Mn $3d$-$3d$ electron Coulomb repulsion $U_{dd} = 5.1 \pm 0.5$ eV, whereas for the valence-band emission calculations, the following parameter values have been used: $pd\sigma = -1.1 \pm 0.25$ eV, $\Delta = 2.0 \pm 0.5$ eV, $U_{dd} = 5 \pm 0.5$ eV while the values for the Racah parameters in the ground state where $B = 0.119$ eV and $C = 0.421$ eV. The crystal-field splitting $10Dq$ was 0.4 eV. With these parameters we calculated the spectrum of Fig. 2. As can be observed in the projected intensity plots, states at low BE (B) receive a large contribution (about 80%) from charge-transfer screened configurations ($|3d^5\underline{L}\rangle$), indicating that a relevant degree of hybridization between Mn and Te levels occurs in this spectral region, whereas states below peak A, have a larger $|3d^4\rangle$ character. However, unlike other systems such as CuO,[34] where the resonating states are found in a narrow-energy region, the Mn RSW in the present compound is spread all over the VB region. Therefore, our photoelectron diffraction analysis of valence-band emission (see below) will be carried out by integrating the photoelectron current over the whole ($\sim$0–10 eV) valence-band energy range.

In order to investigate possible relationships between electronic states in the valence-band region and structural properties of the local Mn environment we carried out a RESPED experiment on the resonating valence-band states (sum of the intensities of peak A, B, and C in Fig. 2) measured for a photon energy at the maximum of the L_{III}-edge resonance (640.5 eV). In addition, the Te $4d$ and Cd $4d$ shallow core lines have also been collected at the same photon energy. The angle-resolved photoemission intensity $I(\theta,\phi)$ was measured for polar angles θ down to 70° from the normal to the surface and for azimuthal angles ϕ over a range of 100° including the two symmetry directions [001] and [1$\bar{1}$0]. We consider the azimuthal anisotropy function $\chi(\theta,\phi) = [I(\theta,\phi)/I_0(\theta,\phi) - 1]$, where $I_0(\theta,\phi)$ is obtained for each azimuth ϕ as a polynomial fit of the polar scan. A plot of χ over (θ,ϕ) is called PED pattern. The RESPED experimental pattern is shown in Fig. 3(h). This pattern has been compared with those calculated for Mn in the CdTe crystal structure [Figs. 3(a)–3(e)]. In the simulations we considered an unrelaxed CdTe(110) crystal structure, with one Mn atom substituting a Cd one [Figs. 3(a)–3(d)], and with one Mn atom in the interstitial sites [Fig. 3(e)] for each of the first four layers. For the simulations from the Mn atoms the kinetic energy of the photoelectrons has been fixed at 636 eV, corresponding to the maximum of the peak A on resonance. Since the MSCD package cannot take account of the resonant photoemission process, we have approximated it by calculating the direct photoemission from a Mn $3d$ level as emitted wave. This approximation has been recently found to give good results in a similar RESPED experiment.[20]

The experimental PED pattern [Fig. 3(h)] was first compared with the calculated pattern of the substitutional Mn atoms [Fig. 3(d)]. This pattern was obtained by adding and averaging the simulated anisotropies of substitutional Mn up to the fourth layer while the results of calculation for partial additions are shown in Figs. 3(a)–3(c). As can be noticed, as the number of layers increases [from Figs. 3(a)–3(d)], new details appear in the calculated pattern that find a correspondence in the experimental data. For example, the peaks indicated with a light blue dot appear when the second layer is introduced, and the features indicated with a light blue rectangle and the light blue oval appear after the third layer is added. In particular the addition of the fourth layer brings in further details in the central region of the pattern.

Then we considered the role of interstitial Mn, calculating the pattern by adding and averaging the simulated anisotropies up to the fourth layer. A qualitative comparison between the experimental pattern [Fig. 3(h)] and this pattern [Fig. 3(e)] indicates that the interstitial Mn can be ruled out, mostly due to presence of the peaks indicated with a blue circle that are very intense and have no correspondence in the measured pattern. This finding deserves further comments. In the case of (Cd,Mn)Te, Mn can occupy either interstitial or substitutional sites. According to a study on the cation diffusion in MBE-grown CdTe layers,[35] the prevalence of one site over the other is determined by the Cd/Te stoichiometry ratio. Indeed it has been shown that Cd excess favors the diffusion of interstitial Mn, whereas Te excess favors the presence of substitutional Mn. In a previous photoemission study,[26] we have shown that for Mn deposition up to 2 ML, the Cd content decreases more rapidly than the Te content (i.e., the surface shows a Te excess), thereby indicating that we should consider as predominant in our Mn:CdTe interface the mechanism where Mn (substitutional) is replacing Cd atoms.

Furthermore, the substitutional position of the Mn atoms that have diffused below the surface can also be inferred by a comparison of the RESPED pattern [Fig. 3(h)] with that obtained from Te $4d$ [Fig. 3(f)] and Cd $4d$ [Fig. 3(g)] shallow core-level lines. In particular, the measured Te $4d$ PED pattern appears to be less compatible with the valence-band RESPED pattern than the Cd $4d$ pattern, indicating that Mn atoms are found in the same local crystalline environment of Cd atoms. For instance, the measured PED pattern for Cd in the regions marked by the light blue dot and the blue circle is quite similar to the Mn RESPED pattern while presenting relevant differences with respect to the Te pattern. It should be noted that some differences between the experimental pat-

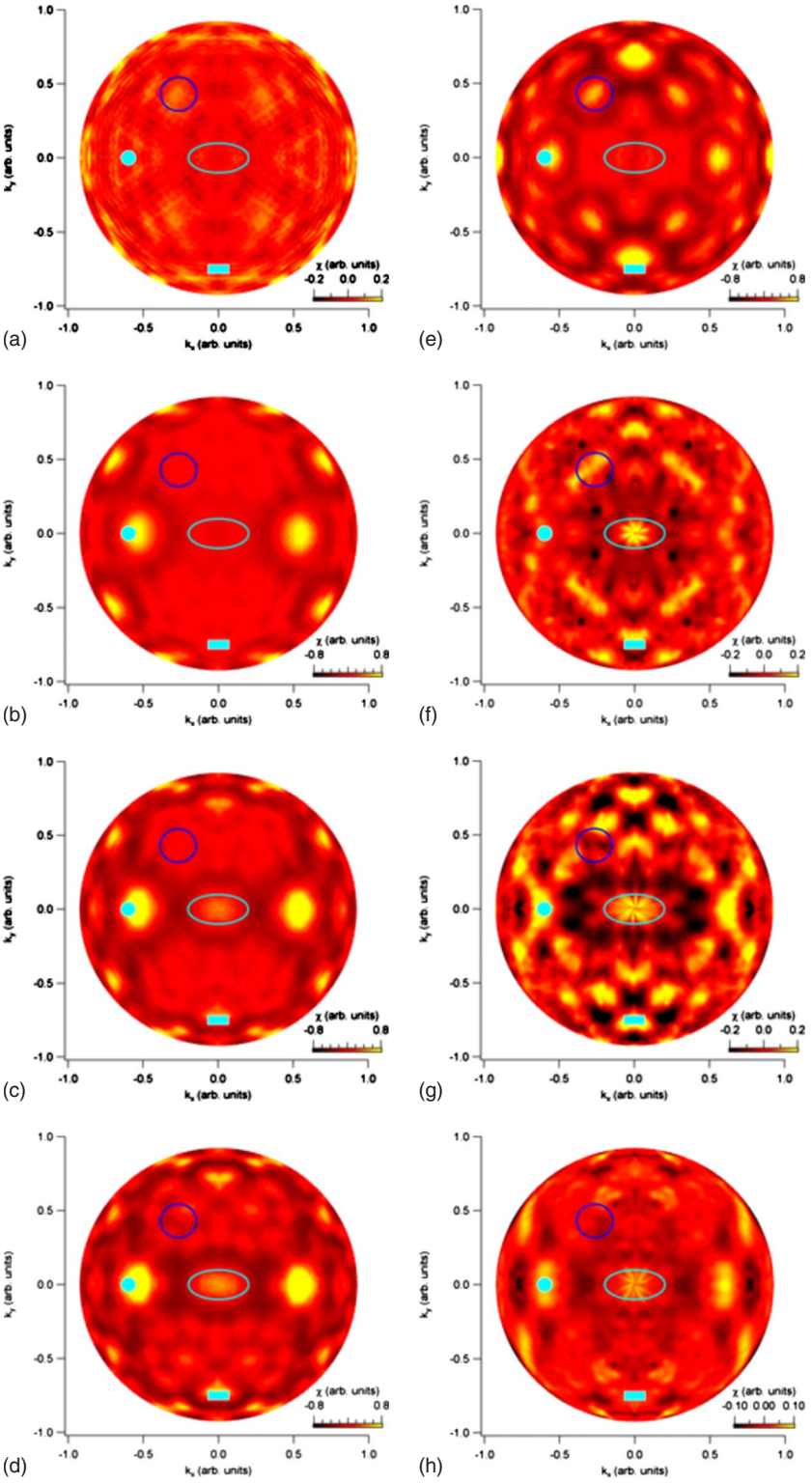

FIG. 3. (Color online) Calculated anisotropies χ for the substitutional Mn atom in different layers. (a) First layer, (b) sum of first and second layers, (c) sum of first to third layers, (d) sum of first to fourth layers, and (e) calculated interstitial Mn atoms (sum of first to fourth layers), (f) measured anisotropy from the Te 4*d* shallow-core levels (photoelectron kinetic energy=594.5 eV), (g) measured anisotropy from the Cd 4*d* shallow-core levels (photoelectron kinetic energy=627 eV), (h) measured anisotropy obtained by considering the signal integrated over the resonantly enhanced valence-electron emission.

tern and the best simulated one can be related to small, but significant in the photoemission intensity, variations of the photon energy during the measurement (yielding enhanced variations of the intensity because of the critical resonating conditions), to the assumption of a nonrelaxed surface and to the approximation of the initial state of the photoelectron with a pure *d*-like state.

In conclusion, we have reconsidered the problem of the Mn:CdTe interface formation at the light of a novel application of the PED technique, supported by a thorough analysis of valence band and Mn core-level data through a CI impurity cluster model. We studied the Mn:CdTe(110) interface obtained by evaporating at RT Mn ions on a CdTe single crystal. It is shown that Mn strongly hybridizes with Te, as probed by Mn core level and resonant valence-band photoemission spectra, while the analysis of resonant PED data

indicates that Mn dilutes inside CdTe at room temperature in a crystalline environment, down to the fourth atomic layer.

Finally, as a future perspective we observe that useful comparisons of the present results could be found with those of atomic layer epitaxy (ALE, see, e.g., Ref. 36 and references therein). Indeed, the deposition of the Mn cations on a CdTe surface is a process that may share several features with ALE, a technique developed to extend the know-how on the growth of CdTe-based SL to ultrathin layers with subnanometer length scale suitably doped with, e.g., Mn or Mg cations. Unlike MBE, where the two constituent elements are brought simultaneously onto the surface, in this technique the cations (Cd, Zn, Mg, or Mn) and anions (Te) are sent alternatively to the sample surface, with a dead time that allows to stabilize the surface and re-evaporate the possible excess material. The choice of relatively high temperatures during the evaporation of single element in ALE of II-VI systems, e.g., typically 280–300 °C,[36] may also trigger interdiffusion processes that can suitably be investigated following the experimental methods depicted in the present study.

[1] S. Oseroff and P. H. Keesom, Semicond. Semimetals **25**, 73 (1988).

[2] M. Bertolini, W. Maslana, H. Boukari, B. Gilles, J. Cibert, D. Ferrand, S. Tatarenko, P. Kossacki, and J. A. Gaj, J. Cryst. Growth **251**, 342 (2003).

[3] H. Boukari, P. Kossacki, M. Bertolini, D. Ferrand, J. Cibert, S. Tatarenko, A. Wasiela, J. A. Gaj, and T. Dietl, Phys. Rev. Lett. **88**, 207204 (2002).

[4] L. Žutić, J. Fabian, and S. Das Sarma, Rev. Mod. Phys. **76**, 323 (2004).

[5] L. Besombes, D. Ferrand, H. Mariette, J. Cibert, M. Jamet, and A. Barski, Int. J. Nanotechnol. **7**, 641 (2010).

[6] M. Goryca, D. Ferrand, P. Kossacki, M. Nawrocki, W. Pacuski, W. Maslana, J. A. Gaj, S. Tatarenko, J. Cibert, T. Wojtowicz, and G. Karczewski, Phys. Rev. Lett. **102**, 046408 (2009).

[7] S. D. Ganichev, S. A. Tarasenko, V. V. Belkov, P. Olbrich, W. Eder, D. R. Yakovlev, V. Kolkovsky, W. Zaleszczyk, G. Karczewski, T. Wojtowicz, and D. Weiss, Phys. Rev. Lett. **102**, 156602 (2009).

[8] M. Goryca, T. Kazimierczuk, M. Nawrocki, A. Golnik, J. A. Gaj, P. Kossacki, P. Wojnar, and G. Karczewski, Phys. Rev. Lett. **103**, 087401 (2009).

[9] Y. S. Chen, S. Halm, E. Neshataeva, T. Kümmel, G. Bacher, M. Wiater, T. Wojtowicz, and G. Karkzewski, Appl. Phys. Lett. **93**, 141902 (2008).

[10] M. K. Kneip, D. R. Yakovlev, M. Bayer, G. Karkzewski, T. Wojtowicz, and J. Kossut, Appl. Phys. Lett. **88**, 152105 (2006).

[11] J. Okabayashi, T. Mizokawa, D. D. Sarma, A. Fujimori, T. Slupinski, A. Oiwa, and H. Munekata, Phys. Rev. B **65**, 161203 (2002).

[12] T. Mizokawa, T. Nambu, A. Fujimori, T. Fukumura, and M. Kawasaki, Phys. Rev. B **65**, 085209 (2002).

[13] L. Sangaletti, S. Pagliara, F. Parmigiani, A. Goldoni, L. Floreano, A. Morgante, and V. Aguekian, Phys. Rev. B **67**, 233201 (2003).

[14] O. Rader, C. Pampuch, A. M. Shikin, W. Gudat, J. Okabayashi, T. Mizokawa, A. Fujimori, T. Hayashi, M. Tanaka, A. Tanaka, and A. Kimura, Phys. Rev. B **69**, 075202 (2004).

[15] A. Wall, A. Raisanen, G. Haugstad, L. Vanzetti, and A. Franciosi, Phys. Rev. B **44**, 8185 (1991).

[16] C. Zeng, Z. Zhang, K. van Benthem, M. F. Chisholm, and H. H. Weitering, Phys. Rev. Lett. **100**, 066101 (2008).

[17] W. Zhu, H. H. Weitering, E. G. Wang, E. Kaxiras, and Z. Zhang, Phys. Rev. Lett. **93**, 126102 (2004).

[18] L. Sangaletti, E. Magnano, F. Bondino, C. Cepek, A. Sepe, and A. Goldoni, Phys. Rev. B **75**, 153311 (2007).

[19] A. Verdini, A. Cossaro, L. Floreano, A. Morgante, A. Goldoni, D. Ghidoni, A. Sepe, S. Pagliara, and L. Sangaletti, Phys. Rev. B **77**, 075405 (2008).

[20] P. Krüger, S. Bourgeois, B. Domenichini, H. Magnan, D. Chandesris, P. Le Fèvre, A. M. Flank, J. Jupille, L. Floreano, A. Cossaro, A. Verdini, and A. Morgante, Phys. Rev. Lett. **100**, 055501 (2008).

[21] S. Jackson, W. E. Hagston, P. Harrison, J. H. C. Hogg, J. E. Nicholls, B. Lunn, P. Devine, and S. Ali, Phys. Rev. B **49**, 13512 (1994).

[22] W. Grieshaber, A. Haury, J. Cibert, Y. M. d'Aubigné, A. Wasiela, and J. A. Gaj, Phys. Rev. B **53**, 4891 (1996).

[23] V. F. Agekian, N. N. Vasil'ev, A. Yu. Serov, N. G. Filosofov, and G. Karczewski, Phys. Solid State **46**, 1776 (2004).

[24] M. Godlewski, T. Wojtowicz, G. Karczewski, J. Kossut, J. P. Bergman, and B. Monemar, Appl. Phys. Lett. **72**, 1104 (1998).

[25] D. Tönnies, G. Bacher, A. Forchel, A. Waag, and G. Landwehr, Appl. Phys. Lett. **64**, 766 (1994).

[26] L. Sangaletti, S. Pagliara, I. Dimitri, F. Parmigiani, A. Goldoni, L. Floreano, A. Morgante, and V. F. Aguekian, Surf. Sci. **566-568**, 508 (2004).

[27] L. Floreano, G. Naletto, D. Cvetko, R. Gotter, M. Malvezzi, L. Marassi, A. Morgante, A. Santaniello, A. Verdini, F. Tommasini, and G. Tondello, Rev. Sci. Instrum. **70**, 3855 (1999).

[28] A. E. Bocquet, T. Mizokawa, T. Saitoh, H. Namatame, and A. Fujimori, Phys. Rev. B **46**, 3771 (1992).

[29] P. S. Bagus, R. Broer, W. A. de Jong, W. C. Nieuwpoort, F. Parmigiani, and L. Sangaletti, Phys. Rev. Lett. **84**, 2259 (2000).

[30] S. Ueda, A. Sekiyama, T. Iwasaki, S. Imada, S. Suga, Y. Saitoh, W. Giriat, and S. Takeyama, Phys. Rev. B **78**, 205206 (2008).

[31] See, e.g., F. Parmigiani and L. Sangaletti, J. Electron Spectrosc. Relat. Phenom. **98-99**, 287 (1999), and references therein.

[32] K. Cho, H. Koh, J. Park, S.-J. Oh, H.-D. Kim, Moonsup Han, J.-H. Park, C. T. Chen, Y. D. Kim, J.-S. Kim, and B. T. Jonker, Phys. Rev. B **63**, 155203 (2001).

[33] T. Mizokawa and A. Fujimori, Phys. Rev. B **48**, 14150 (1993).

[34] L. H. Tjeng, C. T. Chen, J. Ghijsen, P. Rudolf, and F. Sette, Phys. Rev. Lett. **67**, 501 (1991).

[35] A. Seweryn, T. Wojtowicz, G. Karczewski, A. Barcz, and R. Jakiela, Thin Solid Films **367**, 220 (2000).

[36] H. Mariette, in *CdTe and Related Compounds*, edited by R. Tribuoulet and P. Siffert (Elsevier, New York, 2010), Chap. 3, pp. 99–132.